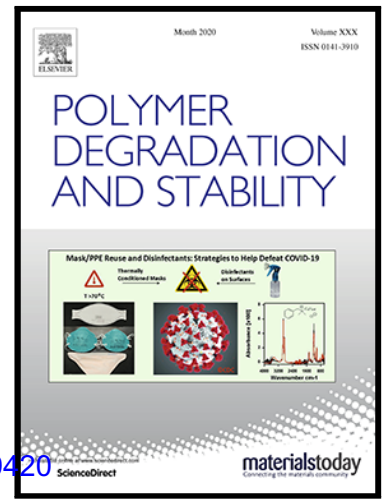

Characterising plasticised cellulose acetate-based historic artefacts by NMR spectroscopy: a new approach for quantifying the degree of substitution and diethyl phthalate contents

Simoní Da Ros , Abil E. Aliev , Isabella del Gaudio , Rose King , Anna Pokorska , Mark Kearney , Katherine Curran

PII: S0141-3910(20)30349-9
DOI: https://doi.org/10.1016/j.polymdegradstab.2020.109420
Reference: PDST 109420

To appear in: *Polymer Degradation and Stability*

Received date: 23 March 2020
Revised date: 7 October 2020
Accepted date: 5 November 2020

Please cite this article as: Simoní Da Ros , Abil E. Aliev , Isabella del Gaudio , Rose King , Anna Pokorska , Mark Kearney , Katherine Curran , Characterising plasticised cellulose acetate-based historic artefacts by NMR spectroscopy: a new approach for quantifying the degree of substitution and diethyl phthalate contents, *Polymer Degradation and Stability* (2020), doi: https://doi.org/10.1016/j.polymdegradstab.2020.109420

Highlights

- ^{1}H NMR for measuring plasticiser loss in cellulose acetate-based historic artefacts
- Degree of substitution determination in plasticised cellulose acetate by ^{1}H NMR
- Assessment of cellulose acetate-based historic artefacts degradation using ^{1}H NMR

Characterising plasticised cellulose acetate-based historic artefacts by NMR spectroscopy: a new approach for quantifying the degree of substitution and diethyl phthalate contents

Simoní Da Ros [†]*, Abil E. Aliev[‡], Isabella del Gaudio[†], Rose King[†], Anna Pokorska[†], Mark Kearney[†], Katherine Curran[†]*

[†] UCL Institute for Sustainable Heritage, University College London, 14 Upper Woburn Place, London WC1H 0NN, United Kingdom.

[‡] UCL Department of Chemistry, University College London, 20 Gordon Street, London WC1H 0AJ, United Kingdom.

* Correspondence author: s.ros@ucl.ac.uk (Simoní Da Ros), k.curran@ucl.ac.uk (Katherine Curran)

ABSTRACT: As one of the first semi-synthetic plastics produced industrially, cellulose acetate (CA)-based artefacts represent valued items in museum collections and archives which, however, present stability issues. High temperature and relative humidity conditions have long been known to promote changes in CA properties, for instance, due to the deacetylation of CA polymer chains and the loss of plasticiser from the polymer matrix. However, there is a need for improved methods for the quantification of plasticiser loss and CA deacetylation. In this context, this contribution presents a new approach for enabling the investigation of plasticiser loss and deacetylation degradation processes in historic plasticised CA-based artefacts which is based on high-resolution proton nuclear magnetic resonance spectroscopy (^{1}H NMR). The proposed methods allow for simple and fast quantification of diethyl phthalate contents and average degree of substitution (DS), while requiring no need for extractive separation between the plasticiser and the CA polymer matrix prior to analysis. Both methods are demonstrated by their application towards a series of reference samples, historic artefacts and artificially aged plasticised CA materials. Our analysis indicates that plasticiser content and DS can be accurately quantified by using high-resolution ^{1}H NMR and both methods have been compared to analyses performed using infrared spectroscopy.

Keywords: cellulose acetate; stability; NMR spectroscopy; plasticiser loss; deacetylation; degree of substitution.

1. Introduction

Cellulose acetate (CA) is a polymer derived from the acetylation of cellulose which finds industrial applications in a wide range of fields, including the production of cigarette filters, textile and fibers, plastics, coatings, photographic films, protective films in liquid crystalline displays, adsorbents and membranes for separation applications [1–4].

As one of the first semi-synthetic plastics produced industrially in the early 20th century and owing to the social impact caused by the advent of polymers, many CA objects, including the sculptures made by Naum Gabo, Antoine Pevsner and László Moholy-Nagy, are collected, conserved and cared for in museum collections and archives, as iconic and valued representations of the past. However, many of these materials present stability issues associated with their chemical and physical degradation, imposing a challenge for conservators in the search for optimal storage and display conditions [5–8].

Both the loss of plasticisers and deacetylation have been described as important processes associated with the loss of structural integrity and aesthetic value of CA art objects [9,10]. Whereas the loss of plasticisers may be linked to physical changes such as warping, crazing, cracking and brittleness [11], the deacetylation of CA chains as a product of hydrolysis is associated with the formation of acetic acid and its release to the environment, resulting in a characteristic vinegar smell, which may further damage materials in the object's vicinity [12].

Given the potential negative impact of these processes on an artefact's historic, aesthetic or information value, developing suitable analytical methods for investigating these processes and their relationship with storage conditions is of paramount importance for protecting cultural heritage, to either expand the life time of artefacts, determine when restoration must take place or define when storage and display conditions must be changed.

Different analytical methods have been proposed for investigating plasticiser loss from CA based materials, for which diethyl phthalate, dimethyl phthalate, triphenyl phosphate and their mixtures are commonly used as external plasticisers [13–15]. Usually, suitable solvents are employed to extract and separate plasticisers from the CA polymer matrix, allowing for the analysis of the solvent-plasticiser solution by either high performance liquid chromatography (HPLC) [13], gas chromatography [16–18] or gravimetry [19]. Alternatively, the weight loss from the polymer phase after extraction has also been used to quantify plasticiser contents [20,21]. In the absence of extraction procedures, plasticiser contents have also been quantified directly in the plasticised CA matrix by either thermogravimetry [1,20,22] or infrared spectroscopy [1,22].

The deacetylation process, in turn, can be studied by quantifying the average degree of substitution (DS), defined as the average number of acetyl substituent groups per anhydroglucose unit (AGU) in the CA molecular structure [23]. For this purpose, a saponification reaction followed by titration of the unreacted NaOH with an acid is a standard recommendation [24–26]. The quantification of the CA saponification product by ion chromatography [17] and additional derivatisation methods, involving the aminolysis of CA followed by gas chromatography-mass spectrometry analysis [20], have also demonstrated promising performance for quantifying DS.

Whereas both plasticiser loss and deacetylation processes can be indirectly monitored by using the above-mentioned methods, the extractive separation of plasticiser and the CA matrix can lead to long analysis times (days) and involve multiple extraction cycles [17]. On the other hand, the use of plasticised CA in infrared spectroscopic studies may be limited to reference materials, due to the superposition of vibration bands for similar phthalates.

In this context, the use of nuclear magnetic resonance (NMR) spectroscopy represents an efficient alternative to overcome the above-mentioned drawbacks, as the requirement for

plasticiser removal and separation from the polymer matrix can be excluded, as previously demonstrated for the quantification of plasticisers in polyvinyl chloride (PVC)-based medical devices [27]. In addition, while the initial sampling procedure requires an interventive approach with respect to the original object, this analysis technique presents the advantage of involving simple sample preparation, requiring minute amounts of sample from the object and enabling further investigation of the dissolved sample after analysis, which can represent a critical characteristic when access to original material from artefacts is limited, as also pointed out by [28]. However, despite being very common in the field of chemistry, the use of NMR spectroscopy for quantifying polymer degradation processes in the heritage field, particularly in polymeric modern and contemporary art pieces, remains underused.

For instance, high-resolution liquid NMR spectroscopy has been applied to the characterisation of the state of hydrolysis and oxidation of oil painting in works of art by monitoring, as a function of the materials' age, the changes in the molar ratio of tri-, di-, and monoglycerides, and the formation of free fatty acids as a result of hydrolysis [28,29]. Identification and semi-quantitative analysis of the chemical composition of solvent extracts from contemporary art installations based on unsaturated polyester resins has also been demonstrated [30]. Solid-state cross-polarization magic angle spinning (CPMAS) NMR spectroscopy has also been employed in the characterisation of poorly soluble materials, such as ancient natural rubber [31], historical collagen-based parchments [32], oriental lacquers and amber [33], whereas more recently, portable unilateral NMR sensors (NMR-MOUSE) have been successfully used in the quantification of moisture in wall paintings [33,34], plasticisers in PVC [35], and in the monitoring of ageing processes in historic hard rubber [36], low-density polyethylene [37], in addition to other historically significant materials including paper and paintings [38–40].

However, in studies involving historic cellulose acetate artefacts, to the best of our knowledge, high-resolution NMR spectroscopy has been employed only as a qualitative tool for the identification of additives [41], or as a quantitative method for characterising DS in unplasticised, commercial CA samples [42], by using promising ^{1}H and ^{13}C NMR methods previously developed for unplasticised CA [4,43–46]. In this context, while quantitative ^{13}C NMR may present promising performance for quantifying average DS and even allow for the determination of the acetyl distribution in unplasticised CA [46], its use may be complicated by the low natural abundance and low gyromagnetic ratio of the ^{13}C nucleus, which yields much smaller sensitivities when compared to ^{1}H NMR [27,47], and also present the drawback of requiring longer analysis times, due to the long relaxation times and required high temperature [46]. However, the use of high-resolution ^{1}H NMR spectroscopy for quantifying diethyl phthalate (DEP) contents and DS values in plasticised historic CA materials which we report in this paper, including rigorous characterisation of errors from replicated measurements and demonstrated characterisation of spin-lattice relaxation times, has not been reported.

Therefore, this contribution demonstrates for the first time how DEP contents in CA can be quantified using high-resolution ^{1}H NMR spectroscopy while requiring no need for separation between the plasticiser and the CA polymer matrix prior to analysis. In addition, we propose a method for characterising the average degree of substitution of DEP-plasticised CA, also by using high-resolution ^{1}H NMR spectroscopy and requiring no plasticiser removal. Both methods are demonstrated by their application towards a series of reference samples, historic artefacts and artificially aged plasticised CA materials. Our analysis indicates that plasticiser content and CA average degree of substitution can be accurately quantified by using high-resolution ^{1}H NMR and results from both methods have been compared to results obtained by infrared spectroscopy. We envisage this new approach will

prove useful in our and others' continued efforts to determine the effect of aging conditions on CA's aforementioned degradation processes.

2. Materials and methods

2.1 Synthesis of plasticised cellulose acetate

Cellulose acetate (CA) with an average degree of substitution (DS) equal to 2.45 ± 0.05 and diethyl phthalate (DEP) (99.5 %) were purchased from Sigma Aldrich (London, United Kingdom). The purchased CA will be referred to in this text as *Commercial CA*. Plasticised CA samples were prepared using the solvent casting method. To obtain miscible blends and avoid phase separation [14], the amount of plasticiser added was tailored to result in final materials containing no more than 22 wt% of plasticiser. In a typical procedure, plasticised CA containing 20 wt% of DEP was prepared by dissolving DEP (24.12 g) in acetone (100 mL) (99 %, Alfa Aesar), before the addition of *Commercial CA* (96 g), which was then followed by the addition of further acetone (200 mL). The resultant mixture was kept under reflux for 4.5 h with continuous stirring, allowed to cool for 1 h with stirring and finally poured over a flat glass tray.

Slow solvent evaporation was allowed for 1 week by keeping a glass lid over the sample tray at room temperature. The final drying procedure was performed in a vacuum oven (150 mbar) for 96 h at 20 °C. Square sample pieces (2 cm x 2 cm x 2 mm) were produced by cutting and samples were stored at 5 °C prior to ageing experiments and between analyses. Throughout this work, these samples are labelled as *x-DEP/CA*, where *x* represents the plasticiser content in wt%.

2.2 Historic samples

Historic plasticised CA materials, as illustrated in the Figure S1 of the Supporting Information (*SI*), as sheets of five different colours and thickness, were kindly donated by Colin Williamson (CW) and labelled by using the CW initials followed by the colour of the

sheets, as *CW-blue*, *CW-green*, *CW-black*, *CW-brown* and *CW-red*. One additional CA object from the Historic Plastic Reference Collection at the UCL Institute for Sustainable Heritage (HPRC-UCL-SH), named as *HS91* [48], and three historic CA combs, kindly donated by Jen Cruse [49] and labelled as *Comb C1*, *Comb C14* and *Comb C19*, illustrated in Figures S2-S3 of the *SI*, were also evaluated. Finally, two colourful vintage CA pen cases, purchased from private collectors and labelled as *Green Case* and *Blue Case*, Figure S3, were also analysed. Although the manufacturing date of historic samples is uncertain, it is believed that the CW sheets' production was performed between 1960 and 1970, whereas *Comb C14* is dated from 1940.

2.3 Thermal ageing of reference and historic materials

Historic and reference CA materials have been thermally degraded at 40, 55 and 70 °C for different lengths of time which varied between 14 and 120 days. Sample pieces were individually suspended within 100 mL sealed *Duran* glass bottles which contained 20 mL of aqueous sodium bromide saturated solution to produce a relative humidity (RH) of 50% [50]. The control of temperature was performed by placing sample bottles in *Carbolite* ovens. Temperature and relative humidity were monitored during the experiments by using *TinyTag Ultra2*® dataloggers, which were also individually suspended in sealed glass bottles containing the salt saturated solution and kept in the oven.

2.4 NMR spectroscopy

For all NMR analyses, deuterated dimethyl sulfoxide (DMSO-d_6, 99.9 atom % D, Sigma Aldrich, London, United Kingdom, used as received) was used as solvent. ^{1}H NMR spectra were recorded at 298 K on a Bruker Avance Neo 700 MHz NMR spectrometer equipped with a helium-cooled broadband cryoprobe, using a standard single pulse experiment with a 30° pulse (zg30 in the standard library of Bruker NMR pulse sequences). The acquisition time was 4 s and the number of scans was equal to 32. Fourier transformation

was performed after using the exponential window function with line broadening factor equal to 0.3 Hz, followed by phase and baseline correction using the TopSpin software, version 4.0.3. All ^{1}H chemical shifts are referenced to the residual DMSO solvent signal at 2.50 ppm.

2.4.1 Diethyl phthalate plasticiser content quantification

Diethyl phthalate (DEP) plasticiser content quantification was performed by using a certified reference material, 1,2,4,5-tetrachloro-3-nitrobenzene (99.82 %, Sigma Aldrich) as an internal standard (IS), chosen due to its suitable chemical shift which does not overlap with CA or DEP resonances. An accurately weighed amount of plastic sample (25 mg, in small pieces removed with scalpel) was added to 2 ml of DMSO-d_6, followed by sonication of the mixture for 1 h in a sealed glass vial, leading to the complete dissolution of the sample, as illustrated in the Figure S4 of the *SI*. 150 µl of a solution of IS in DMSO-d_6 (106.5 mg·ml^{-1}) was added to 650 µl of the above resultant sample solution before being transferred into 5 mm NMR tubes and analysed.

Spectra were acquired with a recycle (interpulse) delay of 54 s (including acquisition time of 4 s). In order to assess possible relaxation effects on quantitative NMR measurements, spin-lattice relaxation times (T_1) were determined by using the inversion recovery experiment, as detailed in the *SI*. The measured T_1 values for the resonance signals from the IS and the DEP plasticiser were equal to 10.6 and 2.6 s, respectively. As the usual requirement for quantitative analysis involves the use of recycle delays longer than 5 × T_1 for 90° pulses, the recycle delay of 54 s was more than sufficient to allow for the full recovery of the magnetization after the 30° pulse used in this work.

The DEP content (in wt%) was determined using Eq. (1) [51], where I_{DEP,CH_3} and I_{IS} represent the integral intensities obtained for the DEP methyl triplet, calculated between 1.40 and 1.15 ppm, and the IS singlet resonance, calculated between 8.57 and 8.37 ppm,

respectively; N_{DEP} and N_{IS} represent the number of nuclei in the DEP and IS molecules associated with the above resonances, equal to 6 and 1, respectively; M_{DEP} and M_{IS} are the molecular masses of DEP and the IS, in g·mol^{-1}, respectively; m_s and m_{IS} represent the mass of sample and IS, respectively; and, finally, P_{IS} denotes the IS mass fraction purity.

$$DEP\ (wt\%) = \frac{I_{DEP,CH_3}}{I_{IS}} \frac{N_{IS}}{N_{DEP}} \frac{M_{DEP}}{M_{IS}} \frac{m_{IS}}{m_s} P_{IS} \quad (1)$$

The integral intensity for each signal was calculated numerically using the generalized compound trapezoidal rule [52] implemented in Fortran 90, as described in the *SI*. Local baselines, defined by the straight line connecting the extremity points of each integration range, were used for calculating both I_{DEP,CH_3} and I_{IS}, as illustrated in Figure S5(a-b) of the *SI*. The numerical procedure of integration was employed to ensure a fully standardised method of spectra processing, minimising the chances for human error from manual integration within the NMR processing software, and also to allow the simultaneous analysis of multiple spectra. Figure S6 in the *SI* illustrates a typical workflow employed in the above algorithm. Estimated absolute errors of integration were in the range between $1.2 \cdot 10^{-6}$ and $5.0 \cdot 10^{-4}$ among calculated areas and ratios of integral intensities, as also detailed in the *SI*. Additionally, the implementation of the above algorithm allowed for an improvement in the accuracy of calculated ratios of integral intensities when compared to ratios computed using common NMR processing software and/or curve fitting procedures, as also detailed in the *SI*.

2.4.2 Average degree of substitution (DS) quantification

^{1}H NMR samples for analysis were prepared by adding 750 µl of the DMSO-d_6 solvent to about 30 mg of solid plastic. The mixture was allowed to dissolve for 24 h in a sealed glass vial before being transferred to an NMR tube and analysed. Spectra were acquired using a recycle delay of 5 s. Spin-lattice relaxation times (T_1) for CA protons were

found to be similar, between 2.99 and 3.05 s, and the use of longer recycle delays was verified to result in no impact on the quantified DS values, as detailed in the *SI*.

The degree of substitution was calculated using Eq. (2) [3], in which I_{acetyl} represents the integral intensity for the acetyl methyl signal, measured between 2.3 and 1.6 ppm by using Eq. (3), and I_{AGU} represents the integral intensity associated with the glycosidic ring resonances, calculated between 5.75 and 3.40 ppm by using Eq. (4).

$$DS = \frac{7}{3}\frac{I_{acetyl}}{I_{AGU}} \quad (2)$$

$$I_{acetyl} = \left(I_{total,1} - I_{AcOH}\right) \quad (3)$$

$$I_{AGU} = \left(I_{total,2} - I_{DMP} - I_{DEP,CH_2}\right) \quad (4)$$

When present, the signal area from the methyl protons of acetic acid, I_{AcOH}, was calculated between 1.917 and 1.897 ppm, using a local baseline, and subtracted from the total area obtained for the acetyl methyl range, $I_{total,1}$, between 2.3 and 1.6 ppm, Eq. (3). Similarly, in the presence of dimethyl phthalate (DMP), the DMP methyl integral intensity, I_{DMP}, was calculated between 3.825 and 3.812 ppm, using a local baseline, and subtracted from the total area obtained for the glycosidic ring protons range, $I_{total,2}$, between 5.75 and 3.40 ppm, Eq. (4). The integral intensity for the DEP methylene protons signal, I_{DEP,CH_2}, was calculated using Eq. (5), where I_{DEP,CH_3} represents the integral intensity obtained for the DEP methyl triplet, calculated between 1.40 and 1.15 ppm.

$$I_{DEP,CH_2} = \frac{4}{6} \cdot I_{DEP,CH_3} \quad (5)$$

The integral intensity for each signal was calculated numerically as described in the previous section, but local baseline corrections were applied for calculating I_{AcOH}, I_{DMP} and I_{DEP,CH_3} only, as illustrated in the Figure S5 of the *SI*. Figure S7 in the *SI* illustrates a typical workflow employed for spectra processing and calculation of DS.

2.5 Attenuated total reflectance - Fourier transformed infrared spectroscopy (ATR-FTIR)

Infrared spectra were recorded in the frequency region between 4000 and 400 cm^{-1} in a Bruker Platinum-ATR-FTIR equipped with a diamond cell. Sixty-four scans were collected and averaged using a spectral resolution of 4 cm^{-1}. Spectra were baseline corrected by fixing the average absorbance obtained between 2000 and 2200 cm^{-1} at zero before the extraction of individual band intensities. Given the small penetration depth from ATR-FTIR measurements, in order to obtain spectra representative of the sample bulk, all measurements were performed on cross-sectioned slices removed from the sample using a scalpel, in which the external exposed layer was excluded. At least five different cross-sectioned slices were analysed for the characterisation of experimental fluctuations.

2.5.1 Plasticiser content and average degree of substitution quantification

Diethyl phthalate contents were quantified by ATR-FTIR employing the ratio between the maximum absorbance intensity observed around 748 cm^{-1} and 602 cm^{-1} [1,53]. CA reference materials containing known amounts of DEP (6, 10, 14, 20 and 22 wt%) were prepared as described in Section 2.1 and analysed in order to obtain a calibration equation which related the infrared ratio to the sample DEP content. *Commercial CA* was analysed to represent *0-DEP/CA*.

DS values were calculated using the ratio between the absorbance intensity observed around 1215 and 1030 cm^{-1}. A calibration equation relating the infrared ratio and DS was built using CA standards with known DS values (2.45, 2.26, 2.08, 1.93, 1.76 and 1.60), which

were prepared by the physical mixture between the *Commercial CA* (DS of 2.45) and a highly purified cellulose powder (DS of 0, purchased from Sigma-Aldrich), as demonstrated by [54].

3. Results and discussion

3.1 Historic CA ^{1}H NMR spectra

Figure 1 (*i-iii*) shows ^{1}H NMR spectra for the historic samples *CW-blue* and *HS91*, obtained as described in Section 2.4.1 (*i*) and 2.4.2 (*ii, iii*), in which the characteristic resonances from the CA structure can be visualised. As illustrated in the Figure S8 of the *SI*, the ^{1}H NMR spectrum for *Commercial CA* is characterised mainly by two resonance regions, which involve signals from the seven protons from the CA glycosidic ring unit, between 5.75 and 3.4 ppm, indicated as (*a*) in Figure 1 (*i-iii*) and also depicted in Figure 2 , and the signal from the acetyl methyl protons, observed between 2.3 and 1.6 ppm [23,43] and indicated as (*b*) in Figures 1 (*i-iii*) and 2.

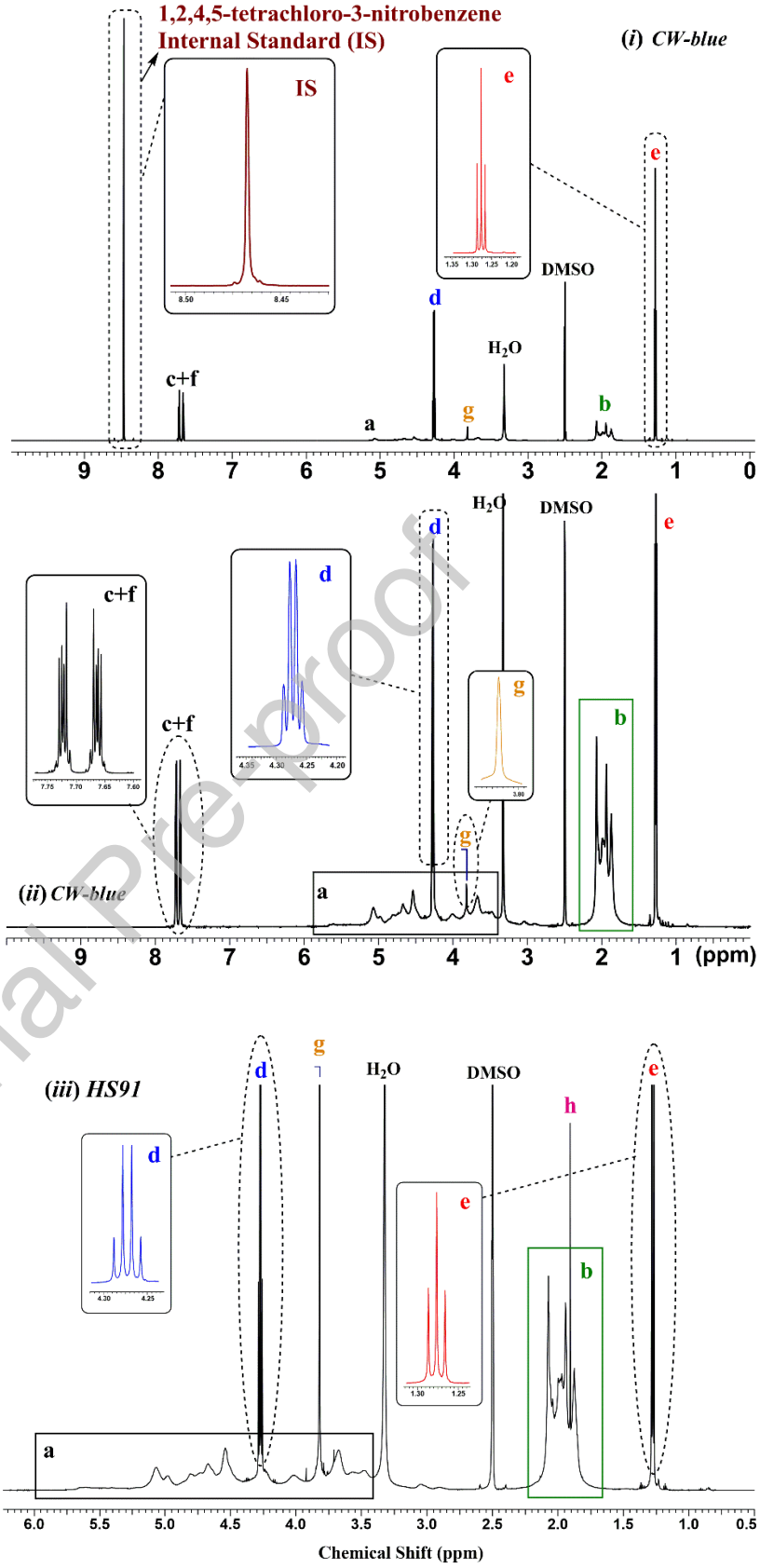

Figure 1 - ^{1}H NMR spectra of the historic *CW-blue* (*i-ii*) and the *HS91* (*iii*) samples (700 MHz, 298 K, DMSO-d_6).

Spectrum (*i*) was obtained as described in *Section 2.4.1* and spectra (*ii*) and (*iii*) as described in *Section 2.4.2.*

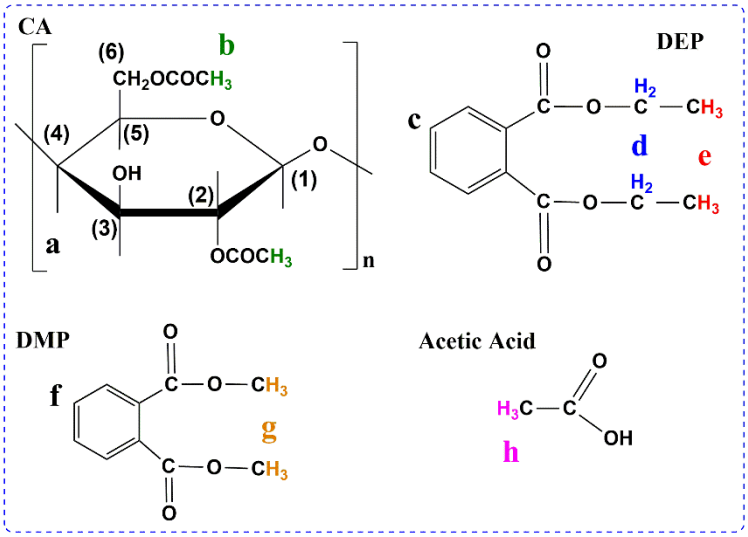

Figure 2 - The structure of the chemical compounds identified in the historic materials.

However, additional resonances have been observed for the different historic CA materials, indicating the presence of additional organic components in their plastic formulation. Diethyl phthalate (DEP) was identified in all samples, as indicated by the presence of resonances at the characteristic chemical shifts from DEP [55], illustrated in Figure S9 of the *SI*, which involve a triplet centered around 1.27 ppm, due to the resonance from the DEP methyl groups, indicated as (*e*) in Figures 1 (*i-iii*) and 2, a quartet centered around 4.27 ppm, due to the resonance from DEP methylene protons, indicated as (*d*) in Figures 1 (*i-iii*) and 2, and two multiplets observed between 7.74-7.70 and 7.69-7.64 ppm, due to the resonances from the DEP aromatic ring, indicated as (*c*) in Figures 1 (*i-ii*) and 2. Additionally, the presence of dimethyl phthalate (DMP) was also identified in some samples, as suggested by the presence of resonances at the characteristic chemical shifts observed for DMP [55], illustrated in the Figure S10 of the *SI*, which involve a singlet around 3.82 ppm, due to the DMP methyl protons, indicated as (*g*) in Figures 1 (*i-iii*) and 2, and two multiplets between 7.76-7.71 and 7.70-7.65 ppm, due to the resonances from the DMP aromatic ring, indicated as (*f*) in Figures 1 (*i-ii*) and 2. This highlights one advantage of NMR spectroscopy as a technique, as it can

unambiguously distinguish between similar additives such as DMP and DEP. The presence of acetic acid was also indicated by the presence of a sharp singlet resonance at 1.91 ppm, Figure 1 (*iii*), characteristic of the methyl group from acetic acid [56], indicated as (*h*) in Figures 1 (*iii*) and 2.

3.2 Plasticiser quantification

Besides allowing for the unequivocal identification of organic additives such as plasticisers in historic artefacts, as demonstrated by this and previous work [41], ^{1}H NMR analysis can also be applied for quantifying their concentrations. In this work, integral intensities from DEP methyl and internal standard signals, obtained from spectra acquired as described in *Section 2.4.1* and illustrated in Figure 1 (*i*), have been used in Eq. (1) to determine the DEP (wt%) content for reference samples, historic artefacts and selected artificially aged plasticised CA and obtained values are summarised and compared to values obtained using ATR-FTIR in Table 1.

Plasticiser contents quantified for the CA reference materials by ^{1}H NMR demonstrated an excellent agreement with the amount of plasticiser added during the sample's synthesis (entries 1-6, Table 1), supporting the validity of the applied methodology. As received historic CA samples presented DEP contents which ranged from 11.78 to 28.10 wt% (entries 7-12, Table 1), whereas selected thermally aged materials presented DEP contents which mostly fluctuated around their initial amount of plasticiser (entries 13-26, Table 1), suggesting that the artificial thermal ageing in sealed environments may have suppressed the loss of plasticiser at these assessed conditions. In general, measurements from selected thermally aged materials suggest that a portion of any plasticiser lost during the initial stages of ageing may have been re-absorbed at longer ageing times as the system approached equilibration. This has been particularly indicated by a slight trend of increase in content observed between 14 and 120 days (see entries 19-21) by both analytical techniques.

Therefore, further studies are needed in order to assess the kinetics of plasticiser loss, which may require either earlier sampling times and/or more severe ageing conditions. However, it should be noted that the investigation of the kinetics of plasticiser loss is beyond the scope of this work.

Table 1 - Quantified diethyl phthalate contents (in wt%) by ^{1}H NMR and ATR-FTIR.

Entry	Sample	^{1}H NMR	ATR-FTIR[a]
Reference CA samples			
1	0-DEP/CA (Commercial CA)	-0.036	0.15
2	*6*-DEP/CA	5.98	5.02 ± 0.27
3	*10*-DEP/CA	9.70 ± 0.01[c]	12.18 ± 0.21
4	*14*-DEP/CA	14.01	11.97 ± 0.15
5	*20*-DEP/CA	21.27 ± 0.65[b]	19.78 ± 0.85[a*]
6	*22*-DEP/CA	22.87	22.25 ± 1.37
As received historic CA			
7	CW-blue	28.07 ± 1.17[b*]	26.91 ± 0.63
8	CW-green	28.10	25.32 ± 0.31
9	CW-black	25.95	24.38 ± 0.59
10	CW-brown	24.73 ± 0.47[c]	23.58 ± 0.26
11	CW-red	21.43 ± 0.20[c]	27.07 ± 0.89
12	HS91	11.78 ± 0.14[c]	23.30 ± 0.69
Artificially aged: historic and reference CA samples			
13	*CW-blue* – (40/14)[d]	26.67 ± 0.33[c]	25.16 ± 0.39

14	*CW-blue* – (40/28)	28.70	26.04 ± 0.84
15	*CW-blue* – (40/120)	28.17	25.21 ± 0.80
16	*CW-blue* – (55/14)	26.33 ± 0.17[c]	24.42 ± 0.75
17	*CW-blue* – (55/28)	26.74 ± 0.12[c]	24.22 ± 0.68
18	*CW-blue* – (55/120)	27.48	23.77 ± 0.57
19	*CW-blue* – (70/14)	26.26 ± 0.21[c]	22.60 ± 1.14
20	*CW-blue* – (70/28)	26.76 ± 0.16[c]	25.19 ± 0.47
21	*CW-blue* – (70/120)	28.91	26.07 ± 0.54
22	*20*-DEP/CA – (40/14)	21.78 ± 0.11[c]	19.49 ± 0.64
23	*20*-DEP/CA – (40/28)	21.79 ± 0.05[c]	19.63 ± 0.32
24	*20*-DEP/CA – (40/120)	18.30	18.63 ± 0.55
25	*20*-DEP/CA – (55/120)	21.78	18.17 ± 0.37
26	*20*-DEP/CA – (70/120)	20.47	17.46 ± 0.40

(a,a*,b,b*,c): Mean and standard deviation from: (a): at least five; (a*): forty eight; (b): four; (b*,c): two measurements. (a,a*,b,b*): Measured using different samples. (c): Measured using same sample. (d): (40/14) Denotes thermal ageing conditions of temperature, in °C, and time, in days, respectively. All thermal ageing experiments were performed at a relative humidity of 50 %.

In addition, a good repeatability was verified (entry 5, Table 1), which was evaluated using different sample pieces and therefore included fluctuations from the plasticiser distribution across the sample. The reproducibility of the method itself was assessed through four replicated measurements performed with the same sample (prepared for NMR), resulting in standard deviations of ± 0.44 %.

To further assess the validity of using high-resolution ^{1}H NMR spectroscopy for quantifying plasticiser contents in historic CA, samples were also analysed by ATR-FTIR, as described in Section 2.5. The quantification of DEP by ATR-FTIR was performed using the

ratio between the maximum absorbance intensity associated to the CH benzene bond vibration from DEP, observed around 748 cm^{-1}, and the CCC ring in-plane deformation vibration from CA, observed around 602 cm^{-1} [1,53], as illustrated in the partial infrared spectra presented in Figure S11 (*i-ii*). As expected, both absorbances features were observed in the plasticised CA reference materials, Figure S11 (*iii-iv*), allowing for their use in the DEP content quantification. Figure 3 shows the resultant relationship obtained between the absorbance intensity ratio and the amount of DEP added in the reference sample synthesis, from which a strong linear correlation could be calculated.

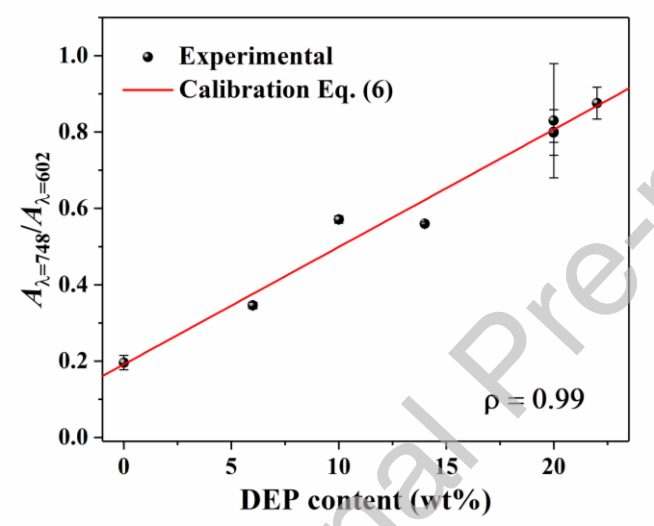

Figure 3 - DEP infrared ratio as a function of the DEP content added in the sample synthesis: experimental infrared ratios (●) and the calibration model Eq. (6) (-). Error bars represent absolute standard deviations.

The coefficients of the linear relationship were calculated by linear regression using the least-square objective function [57], and the resultant calibration equation is presented as Eq. (6), in which A_λ=748 and A_λ=602 represent the maximum absorbance intensity observed around 748 cm^{-1} and 602 cm^{-1}, respectively. Eq. (6) was applied to calculate DEP contents from the infrared spectra of all sample and the results are summarised in Table 1.

$$DEP\ (wt\%) = \frac{\left(\frac{A_{\lambda=748}}{A_{\lambda=602}}\right) - (0.192 \pm 0.0032)}{(0.031 \pm 0.002)} \quad (6)$$

DEP contents calculated from infrared spectra demonstrated an excellent agreement with values quantified by ^{1}H NMR, as shown in Figure 4, which illustrates the linear relationship between DEP contents calculated by the two techniques. It should be noted that results obtained for the *CW-red* and *HS91* historic samples (entries 11-12, Table 1) have been excluded from this comparison (see below). A strong linear correlation coefficient could be calculated as equal to 0.99, supporting the validity of the proposed ^{1}H NMR methodology for characterising DEP contents in historic CA artworks. The excellent agreement between the two techniques is worth noting, as it indicates that issues such as heterogenous plasticiser distribution across historic objects or unavoidable instrumental fluctuations did not lead to significant differences in DEP contents quantified by ^{1}H NMR and ATR-FTIR.

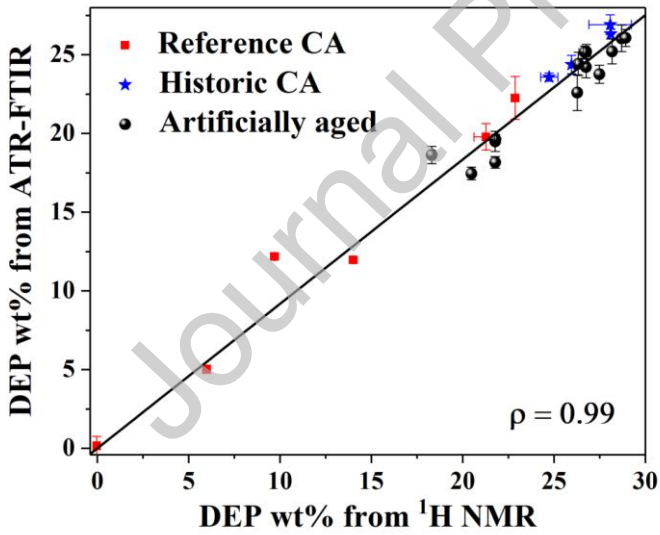

Figure 4 - Linear relationship between DEP content quantified by ^{1}H NMR and ATR-FTIR for the as prepared reference, historic and artificially aged plasticised CA samples. Data is from Table 1, excluding samples *CW-red* and *HS91* (entries 11-12).

As stated above, results obtained for the *CW-red* and *HS91* historic samples (entries 11-12, Table 1) were excluded from the above comparison, as ^{1}H NMR analysis indicated the presence of significant amounts of DMP in these materials, Figure 1 (*iii*). As CH bonds from both DMP and DEP aromatic rings are expected to vibrate at similar infrared frequencies, absorbances observed at 748 cm^{-1} may represent the combined effect from these two plasticisers, resulting in overestimated DEP contents for samples containing a mixture of these phthalates in their composition. Therefore, ^{1}H NMR should be the method of choice for quantifying diethyl phthalate in CA when compared to infrared spectroscopy, as it allows for the unambiguous identification and discrimination between DMP and DEP. On the other hand, the use of infrared spectroscopy for quantitative analysis of these phthalates in CA materials can be only suitable for pure samples of known composition.

3.3 Average degree of substitution (DS) quantification

In order to demonstrate the suitability of ^{1}H NMR for quantifying DS in historic phthalate-plasticised CA, a series of reference samples, historic artefacts and artificially aged plasticised CA were analysed by ^{1}H NMR, as described in *Section 2.4.2*. DS values were then calculated from ^{1}H NMR spectra using Eq. (2) and results are summarised and compared to values obtained using ATR-FTIR in Table 2, along with their associated absolute standard deviations. It is important to note that all samples investigated in this work presented good solubility in DMSO, in agreement with previous research [46].

Values obtained for the *Commercial CA* (entry 2) presented an excellent agreement with the average value provided by the product manufacturer, reported as equal to 2.451 ± 0.05, supporting the validity of the proposed ^{1}H NMR methodology.

Table 2 - Quantified DS by ^{1}H NMR and ATR-FTIR.

Entry	Sample	^{1}H NMR	ATR-FTIR [d]
1	*20*-DEP/CA	2.469 ± 0.022[b]	2.453 ± 0.003
2	Commercial CA	2.476 ± 0.052[a]	2.449 ± 0.009
As received historic CA			
3	CW-blue	2.313 ± 0.022[b]	2.449 ± 0.012
4	CW-green	2.323 ± 0.016[b]	2.457 ± 0.010
5	CW-black	2.268 ± 0.023[b]	2.454 ± 0.012
6	CW-brown	2.256 ± 0.019[b]	2.447 ± 0.009
7	CW-red	2.307 ± 0.026[b]	2.452 ± 0.013
8	HS91	2.219	2.440 ± 0.017
9	Comb C1	1.210	2.380 ± 0.019
10	Comb C14	2.250	2.432 ± 0.001
11	Comb C19	1.564	2.392 ± 0.008
12	Green Case	2.029	2.430 ± 0.015
13	Blue Case	1.987	2.419 ± 0.012
Artificially aged: historic CA			
14	*CW-blue*- 40/14[e]	2.364	2.454 ± 0.018
15	*CW-blue* – 40/28	2.324	2.452 ± 0.014
16	*CW-blue* – 55/14	2.316 ± 0.006[c]	2.444 ± 0.014
17	*CW-blue* – 70/14	2.300	2.452 ± 0.011
18	*CW-blue* – 70/28	2.298	2.450 ± 0.012
19	*CW-blue* – 70/60	2.298	2.444 ± 0.013

20	*CW-blue* – 70/90	2.278	2.438 ± 0.016
21	CW-blue70/120	2.234	2.435 ± 0.012

(a,b,c,d): Average and absolute standard deviation from six (a), three (b), two (c) and at least five (d) measurements. (e): (40/14) Denotes thermal conditions of temperature, in °C, and time, in days, respectively. All thermal ageing experiments were performed at a relative humidity of 50 %.

For historic CA samples, DS values ranged from 1.21 (entry 9, Table 2) to 2.36 (entry 14) and agreed fairly well with the visual state of the artefacts, illustrated in the Figures S1-S3 of the *SI*. For instance, the historic *Comb C1*, Figure S2(c), has demonstrated the most severe visual signs of degradation, such as warping, crazing and a characteristic vinegar smell, in agreement with the lowest DS value quantified by ^{1}H NMR (entry 9). Signs of crazing were also identified in the historic *Comb C19*, Figure S3(a), in line with its DS of 1.56, whereas *Comb C14*, which presented no clear visual sign of degradation, exhibited a DS of 2.25. For the artificially aged *CW-blue* samples, whereas no significant change in DS was observed for samples thermally aged at 40 and 55 °C for 28 and 14 days (entries 14-16, Table 2), a non-linear reduction in the DS values was observed as a function of ageing time at 70 °C (entries 17-21, Table 2), as illustrated in Figure 5, suggesting the loss of acetyl substituent groups from the CA glycosidic units as a result of the ester chain hydrolysis [9,13,21,58] and further supporting the validity of the proposed ^{1}H NMR method for investigating deacetylation processes in historic CA. These results agree with previous research on cellulose triacetate film degradation [10,59], in which an exponential increase on the level of free acidity (and thus a decrease in DS) was observed after approximately 120 days at 70 ˚C and 50% RH.

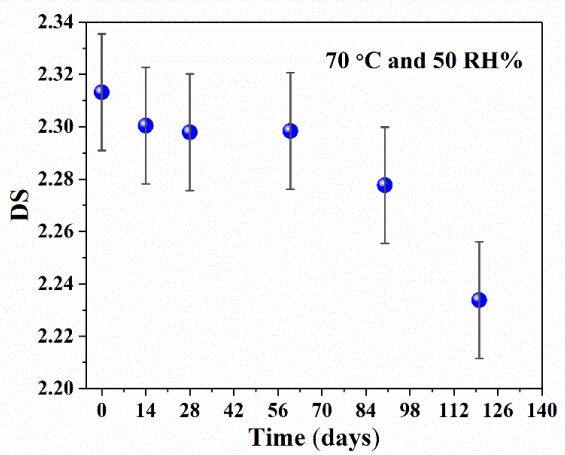

Figure 5 - Average degree of substitution (DS) as a function of ageing time at 70 °C for the *CW-blue* historic CA, as quantified by ^{1}H NMR. Error bars represent absolute standard deviations.

To further evaluate the suitability of the ^{1}H NMR methodology for quantifying DS, samples have also been analysed by ATR-FTIR. The quantification of DS by ATR-FTIR was based on the ratio between the maximum absorbance intensity of the C-O ester vibration, observed around 1215 cm^{-1}, $A_{\lambda=1215}$, and the C-O-C vibration from CA backbone [54,60–63], observed around 1030 cm^{-1}, $A_{\lambda=1030}$, as illustrated in the partial infrared spectra presented in Figure 6.

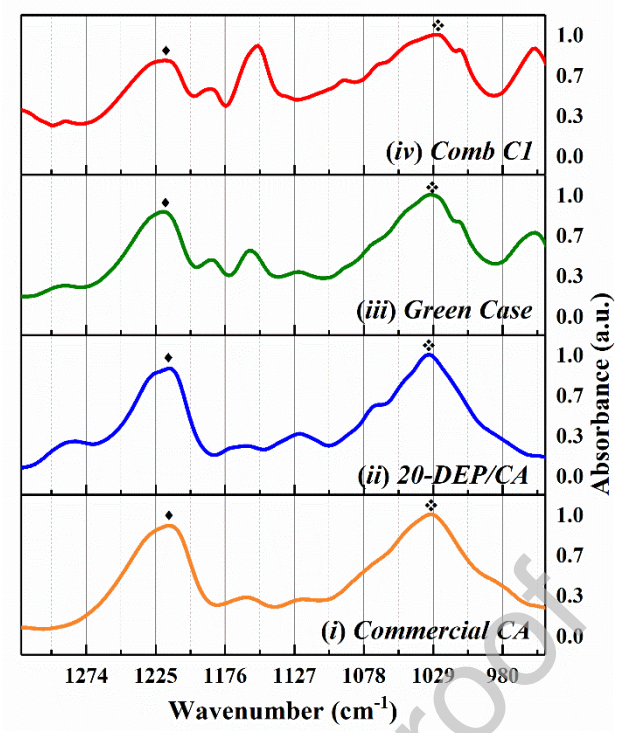

Figure 6 – Partial infrared spectra regions obtained for the *Commercial CA* (*i*), as prepared *20-DEP/CA* reference material (*ii*), the *Green Case* (*iii*) and *Comb C1* (i*v*) historic artefacts. In the figure, (♦) represents the C-O vibration from the CA acetyl substituent group and (❖) denotes the C-O-C vibration from CA backbone.

CA reference samples with known average DS values (see section 2.5.1) were analysed in order to obtain a calibration relating the infrared ratio and DS, as illustrated in Figure 7 and described by Eq. (7). Eq. (7) was then applied to calculate DS values from infrared spectra of all samples and the results are summarised in Table 2.

$$DS = (0.949 \pm 0.047) + (2.574 \pm 0.171) \cdot \left(\frac{A_{\lambda=1215}}{A_{\lambda=1030}}\right) - (0.997 \pm 0.138) \cdot \left(\frac{A_{\lambda=1215}}{A_{\lambda=1030}}\right)^2 \quad (7)$$

Whereas the analysis of the as prepared *20-DEP/CA* reference material and the *Commercial CA* has indicated an excellent agreement between the ^{1}H NMR and ATR-FTIR methods (entries 1-2, Table 2), DS values calculated for historic samples by ATR-FTIR were usually higher than the ones obtained by ^{1}H NMR.

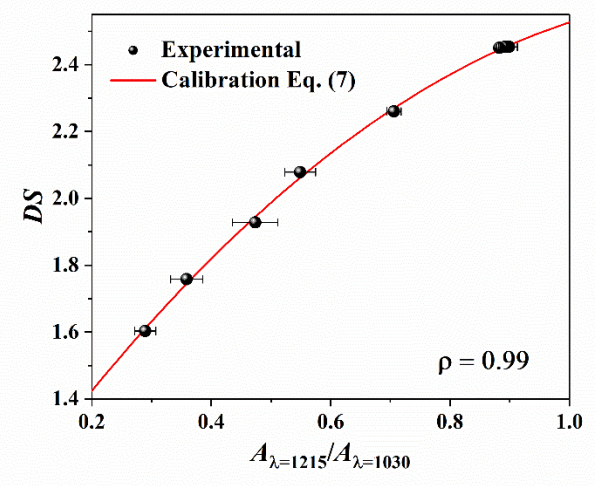

Figure 7 – Average DS as a function of the infrared ratio: experimental infrared ratios (●) and the calibration Eq. (7) (-). Error bars represent absolute standard deviations.

Nevertheless, both methods indicated a similar trend in the observed changes in DS, resulting in a strong linear relationship between DS values calculated between the two techniques, as illustrated in Figure 8, from which a linear correlation coefficient of 0.95 could be calculated. For instance, as observed by ^{1}H NMR, the lowest DS obtained by ATR-FTIR was also associated with the historic *Comb C1* sample (entry 9, Table 2), followed by the historic artefact *Comb C19*, which presented a DS of 2.39 according to the infrared analysis (entry 11), compared with a DS of 1.56 as estimated by ^{1}H NMR.

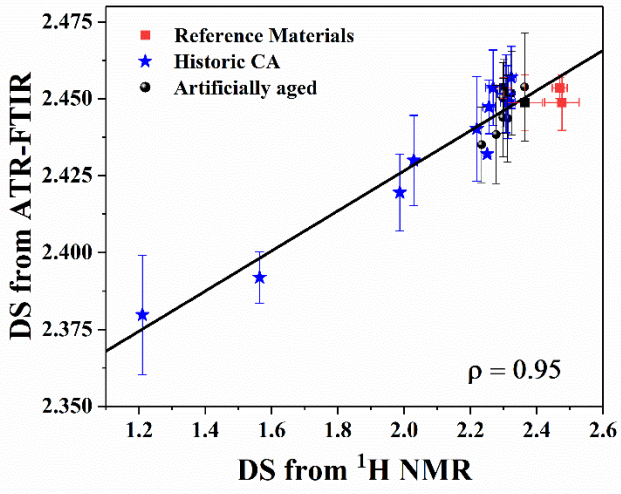

Figure 8 - Linear relationship between DS quantified by ^{1}H NMR and ATR-FTIR for the as prepared reference, historic and artificially aged plasticised CA samples.

Additionally, ATR-FTIR measurements have also suggested smaller DS values for the vintage pen cases *Green Case* and *Blue Case* (entries 12-13, Table 2) when compared to the *CW-colour* samples (entries 3-7, Table 2). However, although ATR-FTIR analysis has supported results obtained by ^{1}H NMR, its use might be complicated by the loss of spectral resolution as CA degrades, as illustrated in Figure 6, in addition to the possible impact of chain scissions and ring opening on the absorbance of the C-O-C signal, which could explain the higher DS values calculated by infrared analysis for more significantly degraded samples. While alternative infrared ratios involving the use of hydroxyl stretching vibrations in the 3480 cm^{-1} region have been proposed for monitoring DS changes in historic CA [9,20], these ratios can be affected by the presence of moisture in the sample, which should be removed prior to analysis. As any drying procedure involving the thermal treatment at high temperatures can result in further loss of acetyl substituent groups, the use of infrared ratios involving hydroxyl bands also seems problematic. Furthermore, it is important to emphasise that whereas infrared spectroscopy can be calibrated for monitoring trends related to changes in the concentration of specific chemical bonds, the use of ^{1}H NMR allows for the direct measurement of the molar proportion between acetate groups and anhydroglucose units in the CA structure, allowing for a more quantitative analysis. This is a key advantage when compared to infrared spectroscopy.

4. Conclusions

This work has presented a new approach towards the characterisation of historic cellulose acetate plasticised with diethyl phthalate, based on high-resolution NMR spectroscopy. The proposed methods have been demonstrated by their application towards a

series of reference samples, historic and artificially aged plasticised CA samples and results have been supported by infrared spectroscopy. Our results show that high-resolution NMR spectroscopy is particularly suited for the analysis of historic plastic materials, as it can be used to analyse samples with complex compositions (e.g. with multiple phthalate additives) and for severely degraded samples.

Unlike conventional infrared spectroscopic methods, our method allows for identifying, discriminating and quantifying diethyl phthalate in CA and provides a more robust method for quantifying the degree of substitution. When compared to other analytical techniques such as GC/MS, there is no need for time-consuming extraction steps prior to analysis, enabling the study of plasticiser loss or deacetylation in CA artworks in a shorter timeframe.

We propose that the use of high-resolution NMR spectroscopy can contribute to ongoing efforts to investigate the impact of environmental storage conditions on the rate of degradation processes associated with plasticiser loss and deacetylation in CA historic plastics.

5. Supporting information

Supporting information (SI) is available presenting additional experimental data and discussion.

6. Notes

The authors declare no competing financial interest.

Declaration of interests

☒ The authors declare that they have no known competing financial interests or personal relationships that could have appeared to influence the work reported in this paper.

7. Acknowledgements

This project has received funding from the European Research Council (ERC) under the European Union's Horizon 2020 research and innovation programme (grant agreement No 716390). We thank Colin Williamson and Jen Cruise for the donation of historic CA. We also acknowledge support by EPSRC (EP/P020410/1) for the 700 MHz NMR facility.

8. Authors contributions statement

Simoní Da Ros: Conceptualization, Methodology, Formal Analysis, Investigation, Writing - Original Draft, Writing - Review and Editing. **Abil E. Aliev**: Methodology, Writing - Review and Editing. **Isabella del Gaudio**: Methodology, Writing - Review and Editing. **Rose King**: Methodology, Writing - Review and Editing. **Anna Pokorska**: Methodology, Writing - Review and Editing. **Mark Kearney**: Methodology, Writing - Review and Editing. **Katherine Curran**: Conceptualization, Methodology, Formal Analysis, Writing - Review and Editing, Funding Acquisition.

9. References

[1] E. Richardson, M. Truffa Giachet, M. Schilling, T. Learner, Assessing the physical stability of archival cellulose acetate films by monitoring plasticizer loss, Polym. Degrad. Stab. 107 (2014) 231–236. doi:10.1016/j.polymdegradstab.2013.12.001.

[2] J. Puls, S.A. Wilson, D. Hölter, Degradation of Cellulose Acetate-Based Materials: A Review, J. Polym. Environ. (2011). doi:10.1007/s10924-010-0258-0.

[3] Y. Cao, J. Wu, T. Meng, J. Zhang, J. He, H. Li, Y. Zhang, Acetone-soluble cellulose acetates prepared by one-step homogeneous acetylation of cornhusk cellulose in an ionic liquid 1-allyl-3-methylimidazolium chloride (AmimCl), Carbohydr. Polym. 69 (2007) 665–672. doi:10.1016/j.carbpol.2007.02.001.

[4] A. El Nemr, S. Ragab, A. El Sikaily, A. Khaled, Synthesis of cellulose triacetate from cotton cellulose by using NIS as a catalyst under mild reaction conditions, Carbohydr. Polym. 130 (2015) 41–48. doi:10.1016/j.carbpol.2015.04.065.

[5] J.-L. Bigourdan, Stability of Acetate Film Base: Acelerated-Aging Data Revisited, J. Imaging Sci. Technol. 50 (2006) 494–501.

[6] K. Curran, A System Dynamics Approach to the Preventive Conservation of Modern Polymeric Materials in Collections, Stud. Conserv. 63 (2018) 342–344. doi:10.1080/00393630.2018.1476959.

[7] J. Bigourdan, J.M. Reilly, Effectiveness of Storage Conditions in Controlling the vinegar syndrome: Preservation strategies for acetate base Motion-Picture Film Collections, in: Proce. JTS, 2000: pp. 14–34. https://www.imagepermanenceinstitute.org/webfm_send/307.

[8] J.K. Atkinson, Environmental conditions for the safeguarding of collections: A background to the current debate on the control of relative humidity and temperature, Stud. Conserv. 59 (2014) 205–212. doi:10.1179/2047058414Y.0000000141.

[9] D. Littlejohn, R.A. Pethrick, A. Quye, J.M. Ballany, Investigation of the degradation

of cellulose acetate museum artefacts, Polym. Degrad. Stab. (2013). doi:10.1016/j.polymdegradstab.2012.08.023.
[10] I.R. Ahmad, D. Cane, J.H. Townsend, C. Triana, L. Mazzei, K. Curran, Are we overestimating the permanence of cellulose triacetate cinematographic fi lms ? A mathematical model for the vinegar syndrome, Polym. Degrad. Stab. 172 (2020) 109050. doi:10.1016/j.polymdegradstab.2019.109050.
[11] Y. Shashoua, Conservation of Plastics, 1st ed., Elsevier Ltd., Oxford, 2008.
[12] K. Curran, A. Možir, M. Underhill, L.T. Gibson, T. Fearn, M. Strlič, Cross-infection effect of polymers of historic and heritage significance on the degradation of a cellulose reference test material, Polym. Degrad. Stab. (2014). doi:10.1016/j.polymdegradstab.2013.12.019.
[13] Y. Shinagawa, Y., Murayama, M., Sakaino, Investigation of the archival stability of cellulose triacetate film: the effect of additives to CTA support, in: and C.V.H. N.S. Allen, M. Edge (Ed.), Polym. Conserv., Cambridge: Royal Society of Chemistry, Cambridge, 1992: pp. 138–150.
[14] C.Y. Bao, D.R. Long, C. Vergelati, Miscibility and dynamical properties of cellulose acetate / plasticizer systems, Carbohydr. Polym. 116 (2015) 95–102. doi:10.1016/j.carbpol.2014.07.078.
[15] J.S. Tsang, O. Madden, M. Coughlin, A. Maiorana, J. Watson, N.C. Little, R.J. Speakman, Degradation of "Lumarith" cellulose acetate, Stud. Conserv. 54 (2009) 90–105. doi:10.1179/sic.2009.54.2.90.
[16] M. Bonini, E. Errani, G. Zerbinati, E. Ferri, S. Girotti, Extraction and gas chromatographic evaluation of plasticizers content in food packaging films, Microchem. J. 90 (2008) 31–36. doi:10.1016/j.microc.2008.03.002.
[17] J. Mazurek, A. Laganà, V. Dion, S. Etyemez, C. Carta, M.R. Schilling, Investigation of cellulose nitrate and cellulose acetate plastics in museum collections using ion chromatography and size exclusion chromatography, J. Cult. Herit. 35 (2019) 263–270. doi:10.1016/j.culher.2018.05.011.
[18] B. Kemper, D.A. Lichtblau, Extraction of plasticizers: An entire and reproducible quantification method for historical cellulose acetate material, Polym. Test. 80 (2019) 106096. doi:10.1016/j.polymertesting.2019.106096.
[19] G.C. Whitnack, E. Clair Gantz, Extraction and Determination of Plasticizers from Cellulose Acetate Plastics, Anal. Chem. 24 (1952) 1060–1061. doi:10.1021/ac60066a054.
[20] M.T. Giachet, M. Schilling, K. McCormick, J. Mazurek, E. Richardson, H. Khanjian, T. Learner, Assessment of the composition and condition of animation cels made from cellulose acetate, Polym. Degrad. Stab. 107 (2014) 223–230. doi:10.1016/j.polymdegradstab.2014.03.009.
[21] N.S. Allen, M. Edge, J.H. Appleyard, T.S. Jewitt, C. V. Horie, D. Francis, Acid-catalysed degradation of historic cellulose triacetate, cinematographic film: Influence of various film parameters, Eur. Polym. J. 24 (1988) 707–712. doi:10.1016/0014-3057(88)90002-X.
[22] D.C. Rambaldi, C. Suryawanshi, C. Eng, F.D. Preusser, Effect of thermal and photochemical degradation strategies on the deterioration of cellulose diacetate, Polym. Degrad. Stab. 107 (2014) 237–245. doi:10.1016/j.polymdegradstab.2013.12.004.
[23] H. Kono, H. Hashimoto, Y. Shimizu, NMR characterization of cellulose acetate: Chemical shift assignments, substituent effects, and chemical shift additivity, Carbohydr. Polym. 118 (2015) 91–100. doi:10.1016/j.carbpol.2014.11.004.
[24] J. Cai, P. Fei, Z. Xiong, Y. Shi, K. Yan, H. Xiong, Surface acetylation of bamboo

cellulose: Preparation and rheological properties, Carbohydr. Polym. 92 (2013) 11–18. doi:10.1016/j.carbpol.2012.09.059.
[25] ASTM - Standard Test Methods of testing Cellulose Acetate, 2010. doi:10.1520/D0871-96R10.2.
[26] M. Nevoralová, M. Koutný, A. Ujčić, P. Horák, J. Kredatusová, J. Šerá, L. Růžek, M. Růžková, S. Krejčíková, M. Šlouf, Z. Kruliš, Controlled biodegradability of functionalized thermoplastic starch based materials, Polym. Degrad. Stab. 170 (2019). doi:10.1016/j.polymdegradstab.2019.108995.
[27] S. Genay, F. Feutry, M. Masse, C. Barthélémy, V. Sautou, P. Odou, B. Décaudin, N. Azaroual, Identification and quantification by 1H nuclear magnetic resonance spectroscopy of seven plasticizers in PVC medical devices, Anal. Bioanal. Chem. 409 (2017) 1271–1280. doi:10.1007/s00216-016-0053-4.
[28] A. Spyros, D. Anglos, Study of aging in oil paintings by 1D and 2D NMR spectroscopy, Anal. Chem. 76 (2004) 4929–4936. doi:10.1021/ac049350k.
[29] A. Spyros, D. Anglos, Studies of organic paint binders by NMR spectroscopy, Appl. Phys. A Mater. Sci. Process. 83 (2006) 705–708. doi:10.1007/s00339-006-3532-1.
[30] G. Stamatakis, U. Knuutinen, K. Laitinen, A. Spyros, Analysis and aging of unsaturated polyester resins in contemporary art installations by NMR spectroscopy, Anal. Bioanal. Chem. 398 (2010) 3203–3214. doi:10.1007/s00216-010-4233-3.
[31] J.B. Lambert, C.E. Shawl, J.A. Stearns, Nuclear magnetic resonance in archaeology, Chem. Soc. Rev. 29 (2000) 175–182. doi:10.1039/a908378b.
[32] A.E. Aliev, Solid-state NMR studies of collagen-based parchments and gelatin, Biopolymers. 77 (2005) 230–245. doi:10.1002/bip.20217.
[33] D. Capitani, V. Di Tullio, N. Proietti, Nuclear magnetic resonance to characterize and monitor cultural heritage, Prog. Nucl. Magn. Reson. Spectrosc. 64 (2012) 29–69. doi:10.1016/j.pnmrs.2011.11.001.
[34] N. Proietti, V. Di Tullio, D. Capitani, R. Tomassini, M. Guiso, Nuclear magnetic resonance in contemporary art: The case of “moon Surface” by Turcato, Appl. Phys. A Mater. Sci. Process. 113 (2013) 1009–1017. doi:10.1007/s00339-013-7729-9.
[35] A. Adams, R. Kwamen, B. Woldt, M. Graß, Nondestructive Quantification of Local Plasticizer Concentration in PVC by 1H NMR Relaxometry, Macromol. Rapid Commun. 36 (2015) 2171–2175. doi:10.1002/marc.201500409.
[36] M. Raue, M. Wambach, S. Glöggler, D. Grefen, R. Kaufmann, C. Abetz, P. Georgopanos, U.A. Handge, T. Mang, B. Blümich, V. Abetz, Investigation of historical hard rubber ornaments of Charles Goodyear, Macromol. Chem. Phys. 215 (2014) 245–254. doi:10.1002/macp.201300629.
[37] Y. Teymouri, A. Adams, B. Blümich, Impact of Exposure Conditions on the Morphology of Polyethylene by Compact NMR, Macromol. Symp. 378 (2018) 1–8. doi:10.1002/masy.201600156.
[38] B. Blümich, Aging of polymeric materials by stray-field NMR relaxometry with the NMR-MOUSE, Concepts Magn. Reson. Part A Bridg. Educ. Res. 47A (2018) 1–4. doi:10.1002/cmr.a.21464.
[39] C. Rehorn, B. Blümich, Cultural Heritage Studies with Mobile NMR, Angew. Chemie - Int. Ed. 57 (2018) 7304–7312. doi:10.1002/anie.201713009.
[40] I. Viola, S. Bubici, C. Casieri, F. De Luca, The Codex Major of the Collectio Altaempsiana: A non-invasive NMR study of paper, J. Cult. Herit. 5 (2004) 257–261. doi:10.1016/j.culher.2003.10.003.
[41] A. Pereira, A. Candeias, A. Cardoso, D. Rodrigues, P. Vandenabeele, A.T. Caldeira, Non-invasive methodology for the identification of plastic pieces in museum environment — a novel approach, Microchem. J. 124 (2016) 846–855.

doi:10.1016/j.microc.2015.07.027.
[42] S. Nunes, F. Ramacciotti, A. Neves, E.M. Angelin, A.M. Ramos, É. Roldão, N. Wallaszkovits, A.A. Armijo, M.J. Melo, A diagnostic tool for assessing the conservation condition of cellulose nitrate and acetate in heritage collections: quantifying the degree of substitution by infrared spectroscopy, Herit. Sci. 8 (2020) 1–14. doi:10.1186/s40494-020-00373-4.
[43] H. Kono, Chemical shift assignment of the complicated monomers comprising cellulose acetate by two-dimensional NMR spectroscopy, Carbohydr. Res. 375 (2013) 136–144. doi:10.1016/j.carres.2013.04.019.
[44] T. Heinze, T. Liebert, Chemical characteristics of cellulose acetate, Macromol. Symp. 208 (2004) 167–237. doi:10.1002/masy.200450408.
[45] C.Y. Chen, M.J. Chen, X.Q. Zhang, C.F. Liu, R.C. Sun, Per-O-acetylation of cellulose in dimethyl sulfoxide with catalyzed transesterification, J. Agric. Food Chem. 62 (2014) 3446–3452. doi:10.1021/jf5002233.
[46] H. Kono, H. Hashimoto, Y. Shimizu, NMR characterization of cellulose acetate: Chemical shift assignments, substituent effects, and chemical shift additivity, Carbohydr. Polym. 118 (2015) 91–100. doi:10.1016/j.carbpol.2014.11.004.
[47] E. Breitmaier, W. Voelter, Carbon-13 NMR Spectroscopy - High-Resolution Methods and Applications in Organic Chemistry and Biochemistry, 3rd ed., VCH Verlagsgesellschaft mbH, Weinheim, New York, 1989.
[48] K. Curran, M. Underhill, J. Grau-Bové, T. Fearn, L.T. Gibson, M. Strlič, Classifying Degraded Modern Polymeric Museum Artefacts by Their Smell, Angew. Chemie - Int. Ed. (2018). doi:10.1002/anie.201712278.
[49] J. Cruse, The Comb - Its History and development, Robert Hale Limited, London, 2007.
[50] L. Greenspan, Humidity Fixed Points of Binary Saturated Aqueous Solutions, J. Res. Natl. Bur. Stand. - A. Phys. Chem. 81 (1977).
[51] E.A. Petrakis, L.R. Cagliani, P.A. Tarantilis, M.G. Polissiou, R. Consonni, Sudan dyes in adulterated saffron (Crocus sativus L.): Identification and quantification by1H NMR, Food Chem. 217 (2017) 418–424. doi:10.1016/j.foodchem.2016.08.078.
[52] J.D. Philip, P. Rabinowitz, Methods of Numerical Integration, 2nd ed., Academic Press, Inc., London, 1984. doi:10.1016/b978-0-12-206360-2.50002-9.
[53] V. Gautam, A. Srivastava, K.P. Singh, V.L. Yadav, Vibrational and gravimetric analysis of polyaniline/polysaccharide composite materials, Polym. Sci. Ser. A. 58 (2016) 206–219. doi:10.1134/s0965545x16020085.
[54] P. Fei, L. Liao, B. Cheng, J. Song, Quantitative analysis of cellulose acetate with a high degree of substitution by FTIR and its application, Anal. Methods. 9 (2017). doi:10.1039/c7ay02165h.
[55] B. Garg, T. Bisht, Y.-C. Ling, Sulfonated graphene as highly efficient and reusable acid carbocatalyst for the synthesis of ester plasticizers, RSC Adv. 4 (2014) 57297–57307. doi:10.1039/C4RA11205A.
[56] G.R. Fulmer, A.J.M. Miller, N.H. Sherden, H.E. Gottlieb, A. Nudelman, B.M. Stoltz, J.E. Bercaw, K.I. Goldberg, NMR chemical shifts of trace impurities: Common laboratory solvents, organics, and gases in deuterated solvents relevant to the organometallic chemist, Organometallics. 29 (2010) 2176–2179. doi:10.1021/om100106e.
[57] S. Da Ros, M. Schwaab, J.C. Pinto, Parameter Estimation and Statistical Methods, Ref. Modul. Chem. Mol. Sci. Chem. Eng. (2017). doi:10.1016/B978-0-12-409547-2.13918-6.
[58] T.S. Allen, N. S., Edge, M., Appleyard, J.H., Jewitt, Degradation of Historic Cellulose

Triacetate Cinematographic Film: The Vinegar Syndrome, Polym. Degrad. Stab. 19 (1987) 379–387.
[59] P.Z.. Adelstein, J.M.. Reilly, D.W.. Nishimura, C.J. Erbland, Stability of cellulose ester base photographic film: part I - laboratory testing procedures, SMPTE J. 101 (1992) 336–346.
[60] George Socrates, Infrared and Raman Characteristic Group Frequencies, 3rd ed., Chichester, 2001.
[61] I.. Skornyakov, V.. Komar, IR spectra and the structure of plasticized cellulose acetate films, J Appl Spectros. 65 (1998) 869–876. doi:10.1007/BF02675748.
[62] L. Cao, G. Luo, D.C.W. Tsang, H. Chen, S. Zhang, J. Chen, A novel process for obtaining high quality cellulose acetate from green landscaping waste, J. Clean. Prod. 176 (2018) 338–347. doi:10.1016/j.jclepro.2017.12.077.
[63] M.E. Vallejos, M.S. Peresin, O.J. Rojas, All-Cellulose Composite Fibers Obtained by Electrospinning Dispersions of Cellulose Acetate and Cellulose Nanocrystals, J. Polym. Environ. 20 (2012) 1075–1083. doi:10.1007/s10924-012-0499-1.

Artwork:

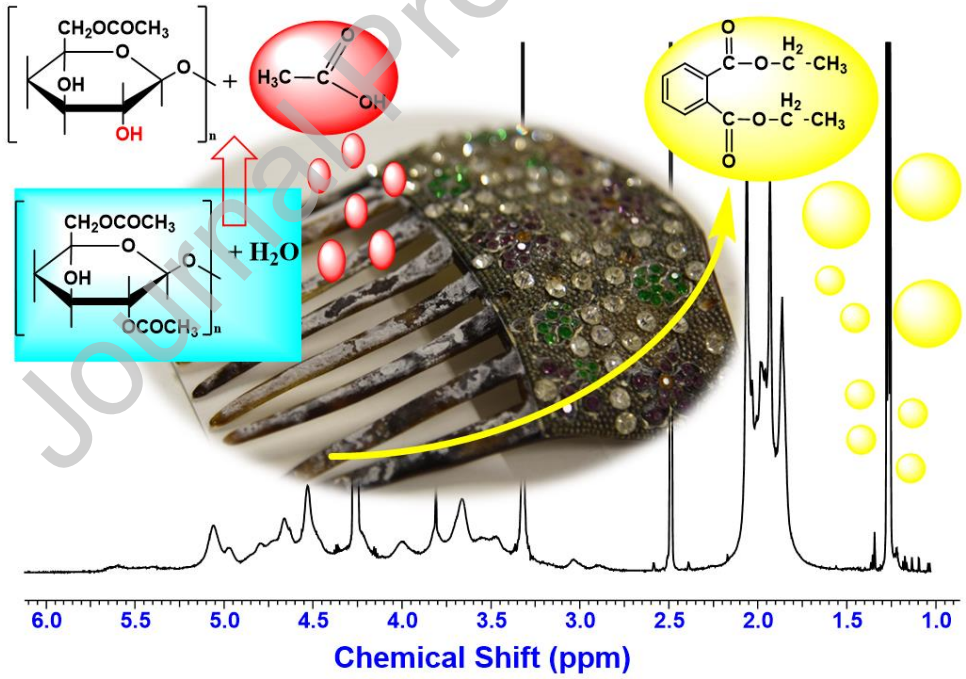

graphical abstract